

## LHCb Vertex Locator Operation Experience

---

**Kazu Akiba**<sup>\*†</sup>

*Nikhef*

*E-mail:* [kazuyoshi.akiba@cern.ch](mailto:kazuyoshi.akiba@cern.ch)

This paper describes the operation of the LHCb's VERtEX LOcator, the VELO in its first year of data taking with a centre-of-mass energy of 7 TeV provided by the LHC machine. The overall performance of the VELO was excellent in this first extended period of data taking. The signal to noise ratio is well above 17, and all the additional infrastructure elements such as the cooling and motion systems behaved well. The radiation damage to the detector is constantly monitored using a few different methods and the observed dose roughly matches the expectations to the LHC collisions.

*The 20th Anniversary International Workshop on Vertex Detectors - VERTEX 2011*

*June 19 - 24, 2011*

*Rust, Lake Neusiedl, Austria.*

---

<sup>\*</sup>Speaker.

<sup>†</sup>on behalf of the LHCb Velo group

## 1. Introduction

The LHCb Experiment [1] is one of the four big experiments currently taking data at the LHC[2] at CERN in Geneva, Switzerland. The LHCb was specifically designed to measure the decays of particles containing  $b$ -quarks produced in high energy pp collisions. At the LHC centre of mass energy regime,  $b\bar{b}$  quark pairs are produced with a large residual boost in the beam axis direction. This fact motivates the asymmetric design of LHCb as a single-arm spectrometer with a high forward acceptance. Due to the relatively long lifetime of the  $b$  hadrons the separation between the primary and secondary vertices is an excellent variable to suppress background events. The precise vertex determination is also crucial for time dependent measurements involving fast meson oscillations, such as those of the  $B_s$ . These factors demand an extremely precise and low material vertex detector.

The Vertex Locator (VELO) is the LHCb's primary and secondary vertex detector and tracking system. It is composed of two detector halves, each one instrumented with 21 modules. Each module is equipped with two semi-circular micro-strip silicon sensors, capable of reading the radial ( $R$ ) and azimuth angle ( $\phi$ ) coordinates. Each sensor (both  $R$ -type and  $\phi$ -type) have 2048 n-type strips implanted on a n-type  $300\ \mu\text{m}$  thick substrate. The strip pitches vary from  $40\ \mu\text{m}$  to  $100\ \mu\text{m}$ . The first active region of the VELO is 8.2 mm away from the beam axis.

## 2. Detector Infrastructure

In order to reach the closest possible distance to the beam collision axis the VELO detector is operated in a secondary vacuum. The VELO vacuum region is separated from the LHC vacuum by the RF-boxes. These boxes, made of a  $300\ \mu\text{m}$  thick Aluminium foil, also minimise beam induction effects over the sensors. The detector vacuum is monitored at all times and has behaved stably over more than a year of operations. The pressure inside the detector vacuum tank is of the order of  $10^{-7}$  mbar, compared to an usual LHC pressure of  $10^{-8}$ – $10^{-9}$  mbar. The plot in Figure 1 shows a typical pressure trend over roughly 2 weeks of standard operation. The power and readout are connected to the modules through feed-through connectors in the vacuum tank. On the inner side of the tank both power, bias voltage and readout are conducted through flexible kapton cables. On the outer side, radiation resistant repeater boards receive the power supplies and re-transmit the readout signals up to the digitisation boards in the safe zone, through approximately 60 m of cables.

The operation under vacuum requires all the heat created by the front-end chips, approximately 20 W per module, to be dissipated with an efficient cooling system while keeping the material budget low. A custom bi-phase  $\text{CO}_2$  cooling system satisfies all these requirements. The detector is kept at an operational set point of  $-30^\circ\text{C}$ , which means approximately  $-8^\circ\text{C}$  at the silicon sensors when the front-end chips are fully configured. Tests of the cooling system were conducted down to the temperature of  $-35^\circ\text{C}$  and no problems were found to operate the system at several different set-point levels (see Figure 2). This temperature is chosen to minimise annealing effects due to radiation damage, while keeping a safety margin to the lowest operational temperature. Long insulated transmission lines were installed from the detector position up to the  $\text{CO}_2$  cooling plant and its controls. The accumulation of ice was noticed nearby the detector tank in the end of one

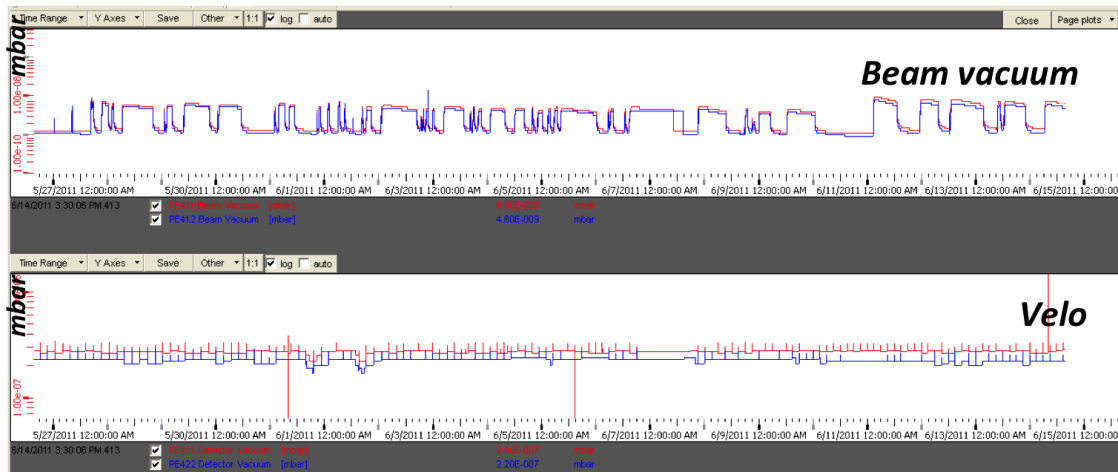


**Figure 1:** The plot shows the monitoring of the VELO vacuum performance (bottom) as well as the LHC vacuum in point 8 (top), LHCb's collision point. The vacuum is in general stable. The fluctuations in LHC's vacuum are related to the presence of the beam. The effect of the presence of the beam is also seen in the VELO vacuum pressure.

of these lines. The ice was formed due to the degradation of parts of the insulating material. The material originally used, Armaflex NH (halogen free), was required to be used as part of CERN safety regulations. The insulation was replaced by the Armaflex AF material on the extremities: nearby the detector tank and the cooling plant, being frequently inspected for ice forming. Along the 55 m transfer line the previous insulation was replaced by foam glass with a thin aluminium cover. Preliminary results indicate that the system is now well insulated. This replacement was performed during the 2010/2011 winter shutdown.

### 3. Power supplies

The high and low voltage power supplies are located in the safe zone, behind the concrete wall. The power to the front-end chips is supplied from a CAEN<sup>1</sup> system and is locally adjusted in regulators residing on the repeater boards. The voltages and currents are permanently monitored and logged, as well as the temperatures in the power regulators (indicating their normal behaviour). No major problems have been found in the low voltage system. The bias voltage to the silicon sensors is provided by an ISEG<sup>2</sup> system. While the front-end are kept powered and configured at all times, apart from machine development periods, the bias voltage is kept off during the injection, ramp and squeezing cycles of the LHC. Only at the final adjust stage the voltages are raised to a standby state, in which only one module on each of the VELO halves is fully depleted. The bias voltage is however quickly ramped (at a 5 V/s rate) as soon as the stable beams flag is announced. This procedure does not cause any additional inefficiency to the data taking, since the detector has

<sup>1</sup><http://www.caen.it/>

<sup>2</sup><http://www.iseg-hv.com/>

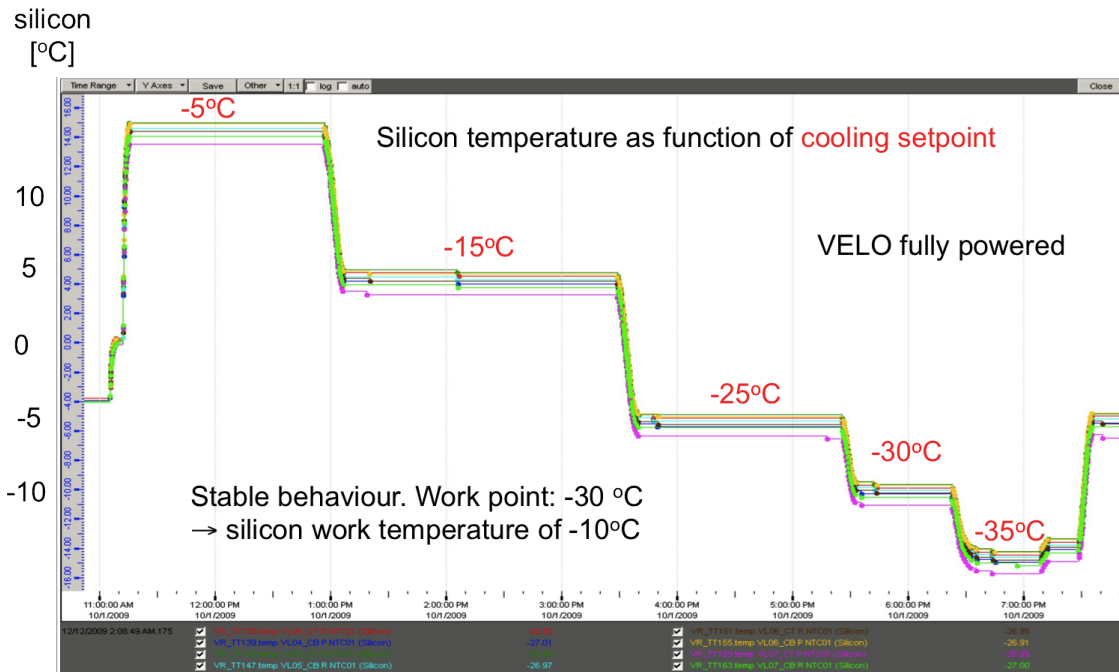


**Figure 2:** Measurements of the temperatures achieved at the cooling blocks while the VELO was fully powered. Several different set point temperatures were tested and the cooling system operates stably down to the temperature of -35 °C. Measurements of the NTC close to the silicon region indicate a temperature of -10 °C at the silicon with the chosen cooling temperature of -30 °C.

also to be closed (see below) and the total time taken by the HV ramping is at the moment very small.

#### 4. Moving system and closing procedure

As previously mentioned the VELO detector remains retracted during the injection period of the LHC. In fact the detector can only begin its closing when the “Movable Devices Allowed in” (MDA) flag is set to true by the LHC, which happens at the same time as the stable beams are declared. At that moment the detector is partially powered and at an opening gap of 58 mm. As of this year the closing procedure, though delicate, is an automated procedure confirmed by the LHCb shift leader.

The VELO closure is performed in four intermediate steps, from the relative distance of each half to the beam of  $x = 29$  mm, to the closed position, the halves pause at  $x = \pm 14$  mm,  $\pm 5$  mm and  $\pm 1$  mm. Figure 3 shows the distribution of the position of the vertices measured during the closing procedure with respect to each of the halves accumulated over several closures, which proves the consistency of the procedure. In each step a newer and more precise image of the beam spot is measured, relative to each half and also in the global LHCb frame. Cross-check measurements are performed at all times (even without collisions) using the potentiometers and resolvers in the movement mechanism.

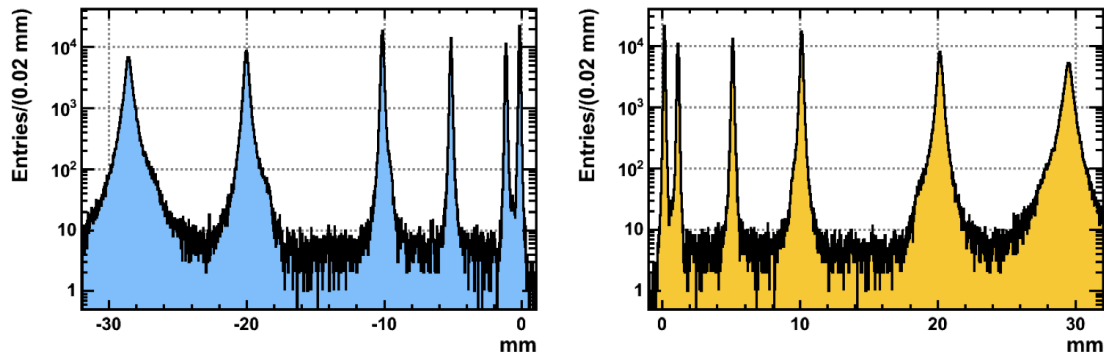


**Figure 3:** The plots show the measurements of the vertices with respect to each VELO half (left and right VELO halves in the corresponding left and right plots). The vertices resolution improves as the VELO gets closer to the beams, which is reflected in the width of the peaks at the intermediate positions where each measurement is taken. Several closures of the VELO are accumulated in these plots which shows the consistency and reproducibility of the procedure.

Overall safety conditions are checked in the beginning, but also monitored at all times during data taking. The silicon bias currents in the sensors are monitored to check for any sharp rises that would be indicative of a large particle flux through the silicon. Two LHC beam condition monitors (BCMs) are used to monitor backgrounds and hence the stability of the beams in proximity to the detector. The procedure will refuse to close the VELO if the BCM threshold is higher than 2% of the LHC beam dump threshold. Additionally, LHCb receives the information from four beam position monitors (BPMs).

Then the actual closing takes place. The VELO reconstructs collision vertices with looser cuts than those of the standard reconstruction. The relative position is calculated for each half and the detector closes symmetrically around the beam spot, including a  $y$  coordinate adjustment.

After closing all the aforementioned conditions are carefully monitored. In addition, the beam vertices are monitored and also checked that a new measurement is received at least every few minutes. The monitoring loop also checks if the DAQ system is running. If any condition is not satisfied the monitoring routine announces the start of a “grace period”. If the underlying cause for the grace period is not solved the VELO is automatically moved out.

## 5. Running conditions of 2010-2011

The nominal LHC filling scheme, with 2808 colliding bunches, was not achieved during the years of 2010 and 2011. On the other hand, a large progress was made on the squeezing of the beams which is capable of considerably raising the instantaneous luminosity. For LHCb this means running in a quite different regime: the detector was designed to acquire events with a single interaction and veto the events with pile up interactions. Offline studies have shown however that it is possible to take relevant data even with several pile-up collisions. The actual data taking limitations reside now in the overall readout speed, the trigger capabilities and the occupancies in the tracking and particle identification detectors. All these factors were combined in selecting running

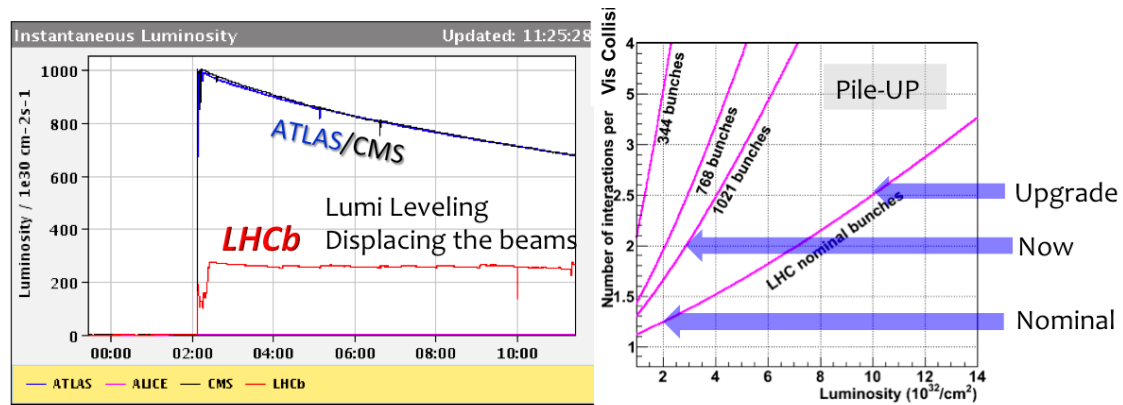


**Figure 4:** The average number of pile-up collisions per event for a few different filling schemes (right). For each scheme there is a maximum instantaneous luminosity that LHCb can take data. As the number of colliding bunches increases the number of pile-up collisions has to be smaller. This is tuned with the luminosity levelling (see text) which is explained on the plot on the left.

conditions of an average collision rate ( $\mu$ ) of about 1.5 collisions per crossing. The luminosity at the LHCb's interaction point is carefully controlled by displacing the beams and therefore reducing the overlap region until this rate is achieved. Figure 4 show a snapshot of the collision rates in each interaction point and illustrate how the luminosity in LHCb is adjusted.

The VELO detector was accurately adjusted to the 50 ns filling scheme set for the LHC running in 2011. The front-end can be time aligned to an accuracy close to 1 ns and the cross-talk to time adjacent 25 ns time samples is around 10%. In fact the equalisation of the cross-talk to the previous and the next 25 ns time sample is the criterion used to align the detectors to the collisions. This time setting is not equivalent to the sampling at the peak of the signal since the rising and falling times are intrinsically different. This choice was made as a trade-off between a symmetric cross-talk in time and a loss in signal to noise ratio of about 5%. Figure 5 shows the result from the combination of all the sensors time aligned and superimposed, showing the overall pulse shape of the VELO.

## 6. Detector Operation

The detector was operated throughout 2010 with the presence of a VELO shifter in the control room in addition to the standard LHCb shift crew of 2 people at all times. The VELO shifter was responsible for powering the detector and for operating the closing procedure. With the detector steadily taking data, the shifter analysed the most recent events checking the non-zero suppressed data as well as the standard zero suppressed stream. In addition a VELO expert was on call for hardware related issues.

The stability achieved in 2010 motivated the operations of the detector without a specific VELO shifter. Extensive work and testing of an automated closing algorithm was performed during the winter break and implemented in the first collisions of 2011. The new procedure performs all the necessary checks and requests the confirmation of the shift leader in a few crucial steps until

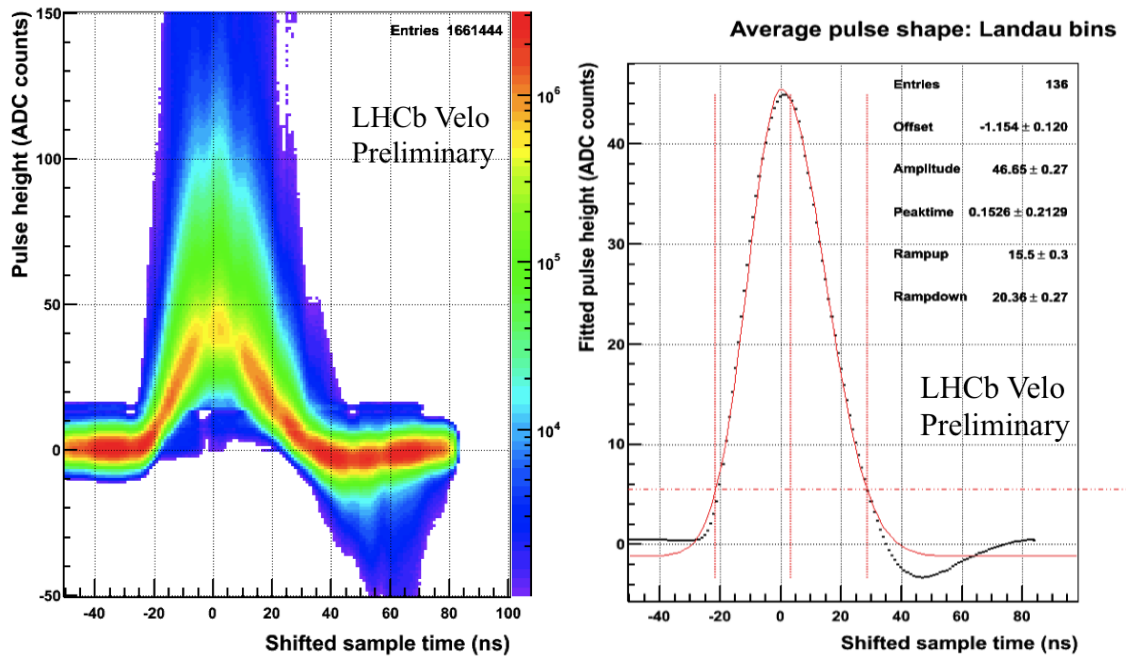


**Figure 5:** The combination of the data from the time alignment scan of all the VELO sensors is shown on the left plot. A Landau function convoluted to a Gaussian is fitted to each time slice and plotted on the right plot. The right plot also shows the fitted function to the pulse shapes, an asymmetric double width Gaussian function. Although this function does not fit well the undershoot, the rising and falling edges are well reproduced by the fit, which are the relevant information for the optimisation algorithm.

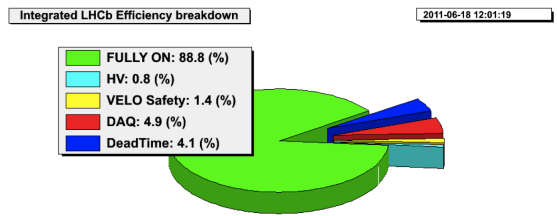


**Figure 6:** The breakdown of the different contributions to the total LHCb data-taking inefficiency. The VELO HV ramp up and closure contribute with a little over 1%.

fully closed. The inefficiency in LHCb operations due to the ramping of the VELO high voltage and the closure of the detector is well below 2% as can be seen in Figure 6.

### 7. Performance

The total luminosity delivered in 2010 (slightly above  $40 \text{ pb}^{-1}$  delivered) was not enough to significantly affect the performance of the sensors. Figure 7 shows the ADC count distribution for

POS(Vertex 2011)008

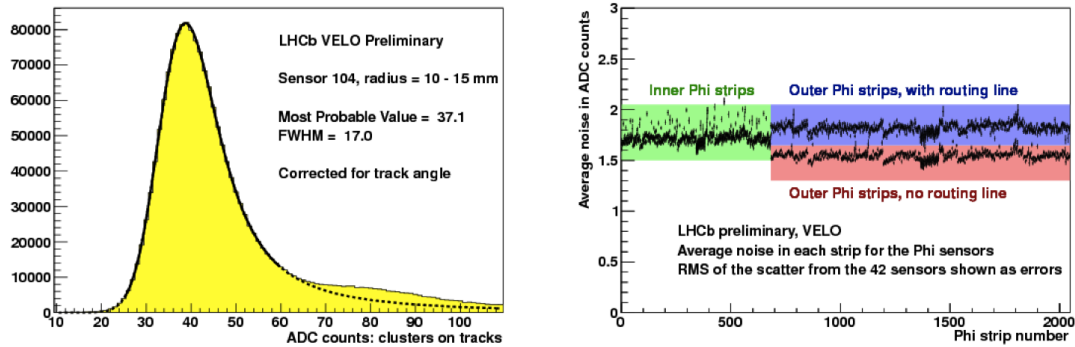


**Figure 7:** On the left plot the distribution of ADC counts for clusters participating in a track for a particular VELO  $\phi$ -sensor. The MPV is around 37 ADC counts. On the right plot the average noise for the  $\phi$ -sensors. The overall average noise is slightly below 2 ADC counts, which gives a signal to noise ratio better than 17.

clusters assigned to tracks for the innermost region of a  $\phi$ -sensor. A Landau convoluted with a Gaussian function is fitted to this distribution which results in a Most Probably Value around 37 ADC counts. The noise levels in both the R and  $\phi$  sensors are shown in Figure 7 and are generally below 2 ADC counts. This leads to a signal to noise performance better than 17 for the whole detector, as per the start of 2011.

## 8. Radiation damage

In 2011 however the total luminosity is much higher than in 2010. The radiation damage is very non uniform in the VELO detector due to its geometry and design. For this reason the radiation damage is monitored with several different methods.

### 8.1 IV curves

Once a week current versus voltage measurements are performed whenever possible (one hour or more without LHC injections). All these curves are kept to trend the evolution of the leakage current as a function of the voltage. Figure 8 shows a plot of the leakage current for an example VELO sensor and also for one of the two n-type strip on a p-type bulk sensors, which shows a very similar radiation damage profile based on the leakage current evolution with the increase of bulk current due to the damage.

### 8.2 Noise versus Voltage

The bias voltage necessary to reach the stable noise conditions changes with the radiation damage. This voltage is related to the depletion voltage but not quite the same, and can be considered as an effective depletion voltage. Measuring the Minimal Noise Voltage (MNV) helps to track the radiation damage in the detector. Here we define the MNV as the voltage necessary to reach 80% of the inverse of the stable noise level ( $1/Noise$ ). In Figure 9 the ratio of the measured MNV at a total integrated luminosity of  $160 \text{ pb}^{-1}$  to the result before the irradiation is shown for different regions of the R-sensors, from closest to further away from the beam axis. In this plot values close



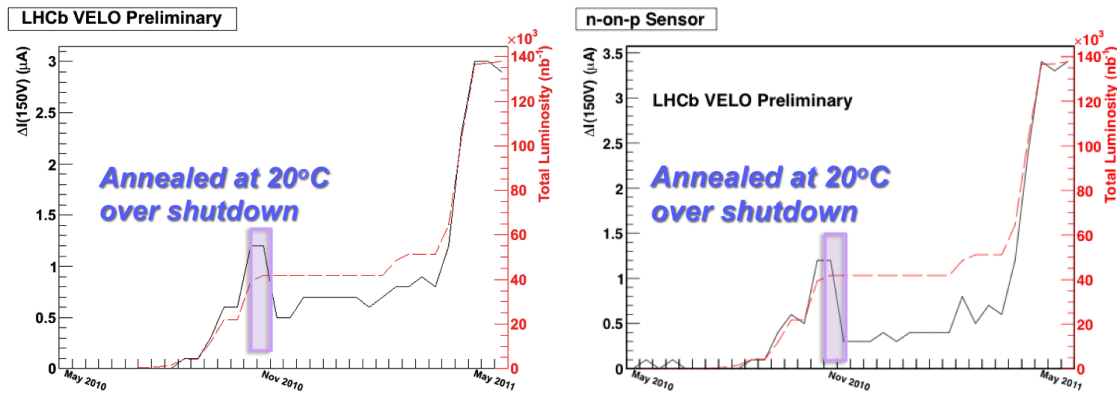


**Figure 8:** On the left plot the monitoring of the leakage current at full depletion voltage for a typical n-on-n VELO sensor. On the right plot the leakage current evolution for one of the n-on-p sensors. The two sensors are at similar distance in  $z$  to the collision point. In summary their performance is very similar.

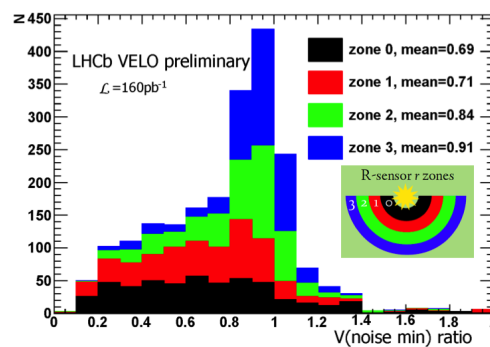


**Figure 9:** The ratio of the Minimal Noise Voltage (MNV) measured in the beginning of the 2011 run and after  $160 \text{ pb}^{-1}$  integrated luminosity, plotted in different colours for different radii regions of the VELO sensors. The MNV is noticeably smaller for the inner regions of the sensors (zone 0) than the outer (zone 3) indicating a reduced depletion voltage due to radiation damage.

to 1 represent no change while values smaller than 1 represent a lower effective depletion voltage, as expected while the sensors are still in the type inversion process.

### 8.3 Charge Collection Efficiency

The charge collection efficiency (CCE) is measured on only a few occasions per year as this requires using collision beam time for a detector dedicated activity. The data for the CCE measurement is taken by scanning the bias voltage applied to one out of 5 modules of the VELO at a time. Several thousands of collision events are recorded for each step. The module being scanned also outputs non-zero suppressed data for each event. The complete scan is composed of 10 steps in voltage and 5 different patterns. The analysis of these data attempts to measure the efficiency of each sensor as a function of voltage while using the other sensors as a telescope. In this way it is also possible to estimate an effective depletion voltage, which in this case is based on the voltage

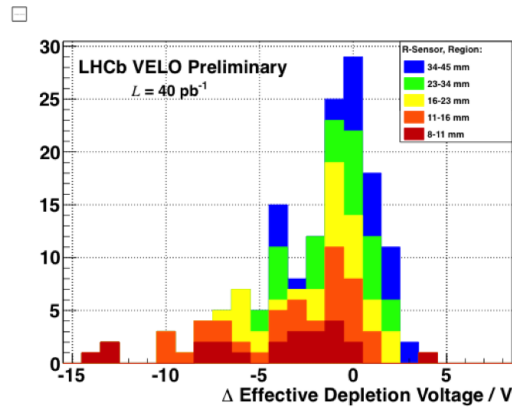


**Figure 10:** The plot shows preliminary results with data from the 2010 CCE analysis. The plot shows the change in the effective depletion voltage, measured at 80% efficiency. The same trend as in Figure 9 is confirmed in this analysis.

when the sensor reaches 80% of its charge collection efficiency. The results of the scan performed in the beginning of 2011 is shown in Figure 10. The change ( $\Delta$ ) of the effective depletion voltage from the scan performed before the start of LHC physics operations is plotted. The total integrated luminosity was only the amount delivered in 2010 of approximately  $40 \text{ pb}^{-1}$ . A similar pattern as in the noise versus voltage scan for different radii regions is observed.

## 9. Summary

During the first year of its physics operation, the VELO detector performed well and no serious operational or performance difficulties were encountered. All its components and subsystems are functioning as expected and in a very stable manner. The  $\text{CO}_2$  cooling and vacuum have performed very stably; no major readout problems were encountered in the power nor in the bias voltage supplies; the detector front-end is operating according to its specifications. The effects of radiation damage are constantly monitored as a function of the integrated luminosity delivered by the LHC machine.

## References

- [1] The LHCb Collaboration *et al*, 2008 JINST 3 S08005 – The LHCb Detector at the LHC
- [2] Lyndon Evans and Philip Bryant, 2008 JINST 3 S08001 – LHC Machine